The potential use of green mussel (Perna Viridis) shells for synthetic calcium carbonate polymorphs in biomaterials

by Rifky Ismail

Submission date: 24-Aug-2021 02:07PM (UTC+0700)
Submission ID: 1635191860
File name: Q2_2021-Crystal_Growth.pdf (4.47M)
Word count: 6944
Character count: 37326

Journal of Crystal Growth 572 (2021) 126282

Contents lists available at ScienceDirect

Journal of Crystal Growth

journal homepage: www.elsevier.com/locate/jcrysgro

The potential use of green mussel (*Perna Viridis*) shells for synthetic calcium carbonate polymorphs in biomaterials

R. Ismail [a,b], D.F. Fitriyana [b,c], Y.I. Santosa [d,e], S. Nugroho [a], A.J. Hakim [a], M.S. Al Mulqi [a], J. Jamari [a], A.P. Bayuseno [a,*]

[a] Mechanical Engineering Dept., Diponegoro University, Semarang, Indonesia
[b] Center for Biomechanics, Biomaterials, Biomechatronics and Bio Signal Processing (CBIOM3S), Diponegoro University, Semarang, Indonesia
[c] Mechanical Engineering Dept., Universitas Negeri Semarang, Semarang, Indonesia
[d] Medicine Department, Diponegoro University, Semarang, Indonesia
[e] Diponegoro National Hospital (RSND), Diponegoro University, Semarang, Indonesia

ARTICLE INFO

Communicated by Keshra Sangwal

Keywords:
A2. Powder processing
A2. Calcination
B1. Green mussel shells
B1. Precipitated calcium carbonates
B1. Biomaterials

ABSTRACT

Green mussel shells contain a high content of calcium that can be potentially used for starting biomaterials. A powder processing and subsequent calcination-dissolution-precipitation (CDP) technique for recycling the shells into the value-added of precipitated calcium carbonates (PCC) is presented in this paper. In the experimental study, the received green mussel shells were initially washed and ground and followed by heat treatment at different temperatures in an electric furnace. PCC product was precipitated from the blended solution of calcium and carbonate ions derived from the heat-treated ground powder. The precipitating solids were then investigated via XRD, SEM-EDX, and FTIR methods. The XRD Rietveld method confirmed that the raw green mussels were rich in crystalline aragonite, which could be recycled into vaterite and calcite in the PCC product. The current study demonstrated that the green mussel shells are technically possible for the starting materials in biomedical applications.

1. Introduction

Green mussels (*Perna Viridis*) are frequently harvested as a food source in the Indo-Pacific region. They are cultivated in coastal waters, mangroves, and river mouths [1]. Normally, the high productivity time of green mussels finds during the peak seasons of March to July [2]. At present, the production of green mussels in Indonesia may reach 309,886 tons/year (data in 2018). If these shells are composed of 70% of the total weight of the mussels, 216,902 tons of waste of green mussel shells require proper disposal in order to reduce environmental pollution. Alternatively, a very large number of these shell wastes could be recycled into added-value products. An attempt has been given in the last decade for processing these shells into the precipitated calcium carbonate (PCC) due to its growing importance as biomedical materials [3]. Due to its high biocompatibility, PCC products could be found in many industrial sectors such as pharmaceutical, biological and biomedical applications [4,5].

In practice, the PCC product with the different polymorphs (i.e., calcite, vaterite, and aragonite) and unique morphology may be synthesized from the mixing of solutions containing calcium ion and carbonate ion depending on the different processing conditions [6–8]. Because of the most stable phase at room temperature, calcite may be easily formed and applied for releasing the targeted and sustainable drugs against cancer cells [9,10]. Due to high solubility in water, however, vaterite is least stable and tends to recrystallize into more stable phases (i.e., calcite or aragonite) depending on the operational conditions [11]. Particularly, spherical vaterite particles are desirable for medical usage relating to their characteristics such as biocompatibility, low toxicity, a high loading volume, and dissolution in relatively mild conditions [12–15]. Additionally, aragonite is the common polymorph of calcium carbonates having an excellent biocompatible property, which is purposed for anti-cancer drug delivery and the scaffolding of bone implants [16–19].

The synthesis of PCC using the different calcium sources of marine wastes (e.g., green mussel shells, shellfish, and animal bones) is now greatly promising [20]. Here the green mussel shells rich in calcium sources offer an option of providing a low-cost raw material for the synthesis of biomedical materials such as the PCC and Ca-

* Corresponding author.
E-mail address: apbayuseno@lecturer.undip.ac.id (A.P. Bayuseno).

https://doi.org/10.1016/j.jcrysgro.2021.126282
Received 27 February 2021; Received in revised form 18 July 2021; Accepted 31 July 2021
Available online 4 August 2021

hydroxyapatite (Ca-HA) product [21–23]. In general, biogenic materials are known as rich in calcium sources and have attractive physico-chemical and biocompatibility characteristics similar to those of human bones [24]. These materials are made of plankton, which dominates the chemical reaction with the carbonate minerals in the surface deposits [25]. For example, the shells of green mussel and oysters contain abundant calcium, varying from 95.7 to 98.2 for CaO (wt.%). It is noted here that results in the form of oxides were provided by XRF analysis independent of the actual form of chemical compounds in the waste shells [26], because light elements such as oxygen and carbon could be not analyzed. However, their cations mainly bind to carbonates. In this case, a range of additional Ca-, Mg-, Mn-, and Fe-rich carbonate minerals are found in the waste shells [25].

In the previous report [27,28] the precipitation route of calcium carbonates is very common through the mixing solution of calcium sources and carbonate ions, while the polymorphs could be controlled with or without chemical additives in varying systems. Specifically, the synthesis factors (e.g., temperature, pH of the solution, reaction time, ion concentration and ratio, stirring, and the concentration of additives) control polymorphs and physicochemical properties of calcium carbonates [27,28].

A great effort to control and manipulate polymorphs of PCC product from shells of blood, cockle, and oyster has been made to-date [29,30]. However, the synthesizing benefits of PCC from the shells of green mussels with a mineral carbonation technology has not yet been fully explored. Correspondingly, the calcination-dissolution-precipitation (CDP) method was proposed for processing shells of green mussels into PCC, depending on a molar ratio of carbonate and calcium ions [26,27]. Understanding of the formation behavior of each polymorphs of PCC and the impacts of the synthesis factors on particle size, shape, density, color, brightness, and other properties required an analytical characterization method (qualitative and quantitative). These analytical tools of capable of distinguishing among the different phases that form during the synthesis are needed.

In the present study, the CDP synthesis of PCC was performed to take advantage of the green mussel shells as a low-cost starting biomaterial. Moreover, the analytical tools (XRD, SEM, and FTIR) were selected for determining the crystalline phases of all three calcium carbonate polymorphs that in turn were used for (i) quantitatively analyzing among the three calcium carbonate polymorphs in a ternary mixture and (ii) examining their morphological developments from the CDP synthesis. These experimental results are expected to provide a benchmark for further synthesis of biomedical material from the biogenic materials specifically the green mussel shells.

2. Materials and method

2.1. Preparation of calcium carbonate samples

The powder processing strategies, including grinding and calcination, was adopted to prepare the waste mussel shells as a bioresource of calcium carbonate. In this experimental study, the calcination of the mussel shells was desirable in view of the possibilities of obtaining pure calcium oxide by removing water, salt, mud, and the remaining meat contained in the mussel shell. It has been demonstrated experimentally [3] that a large scale of shells can be successfully converted through calcination into pure calcium carbonate. The calcination temperatures at both 800 and 900 °C allowed calcium contained in the waste to convert into calcium oxide and carbon dioxide for easing the extraction of calcium ions in acid solution.

Furthermore, the nitric acid solution was employed for dissolving the calcium content of the calcined waste for subsequent PCC synthesis. Subsequently, the dissolution of the calcined waste into the nitric acid was proposed as a simple method for yielding soluble calcium ions, by which the 2:1 M ratio of acid to Ca^{2+} was made by reacting 1 mol of CaO with an excess of nitric acid leading the reaction as follows

$$CaO_{(s)} + 2HNO_3(aq) \rightarrow Ca(NO_3)_2(aq) + H_2O(l) \quad (1)$$

As the main concern of the study is precipitating calcium carbonate (PCC) formation, the crystal forming solution must be in rich Ca^{2+} and carbonaceous species (CO_2, HCO_3^-, CO_3^{-2}), which are crucial and favored under the liquid–vapor equilibrium of CO_2 leading to the formation of different ionic species and pH changes according to

$$Ca^{2+} + CO_3^{2-} \rightarrow CaCO_3 \quad (2)$$

$$Ca^{2+} + 2(HCO^-) \rightarrow CaCO_3 + CO_2 + H_2O \quad (3)$$

$$2HNO_3 + CaO \rightarrow Ca(NO_3)_2 + H_2O \quad (4)$$

Accordingly, such ionic equilibria changes shifted the main species in the solution and the solubility of the calcium carbonate, resulting in its deposition or dissolution [31].

The experimental setup of this research is shown in Fig. 1. As received green mussel shells were initially cleaned using water and subsequently desiccated under the strong sunlight. Moreover, ball milling was applied for reducing the green mussel shell to yield powder which was passed a wire sieve with 100 mesh. This stage yielded raw ground powder material for subsequent calcining at a temperature of 800 °C (Cal-800) and 900 °C (Cal-900) for 5 h using a Carbolite® furnace. For preparing a PCC forming solution was performed by mixing 17 g of the calcined powder in 300 ml of 2 M HNO_3, and the resulted solution was agitated in a magnetic stirrer at 60 °C for 30 min. During the course of the experiment, the NH_4OH was added slowly to provide a pH solution of 12, and the obtained solution was strained using Whatman(42) filter paper. The filtrate was precipitated by slowly flowing CO_2 gas. The resulting milky white precipitate was then cleaned with distilled water to a pH of 7. Eventually, the precipitating solid was recovered by the paper filter and then dried at 110 °C for 2 h. The PCC products with the basic ingredient of raw ground powders have been heat-treated at 800 °C and 900 °C, designated as PCC-800 and PCC-900 samples, respectively. Moreover, FTIR, SEM-EDX, and XRD methods were used to characterize the above samples. Finally, the structural characteristics of the above samples were compared with the results on commercial calcium carbonate powder (Merck, Germany).

2.2. Physico-chemical characterizations of powder samples

For the XRD measurement, an Al-sample holder was fulfilled by the dried powder which was then pressed using the glass slide to ensure that the sample was positioned at the right height. Afterward, the sample was displayed to an x-ray beam in the X-ray diffractometer (Bragg Brentano mode- Philips; PW 3050/60) for recording x-ray spectra. The XRD measurement data (3–80° 2θ, 0.02° steps, and 30 s/step) were taken. Moreover, a search-match program (PC-based match software) was implemented for qualitative analysis of determining each polymorph of calcium carbonates, which was subsequently verified by the XRD Rietveld profile refinements using the Program Fullprof-2 k, version 3.30 [32]. The refinement program used the crystal structure model available in the literature (American mineralogist of crystal structure database AMCSD) [33].

Further quantitative phase analysis of the PCC product was performed using the value of refined scale factor obtained from the Rietveld refinement process, in that the relative weighted fractions of each polymorph (major and minor amounts) of the PCC were determined [34]. In this calculation, a sum of (wt.%) amounts of each crystalline phase must be 100%. The detailed Rietveld refinements of these XRD data are presented elsewhere [35,36]. Additionally, powder samples were examined by the SEM/EDX method for morphology and chemical element analysis. For measurement procedures, the powder samples were initially put on using double-sided conductive tapes on the Al-sample holder and the powder surface was coated with carbon.

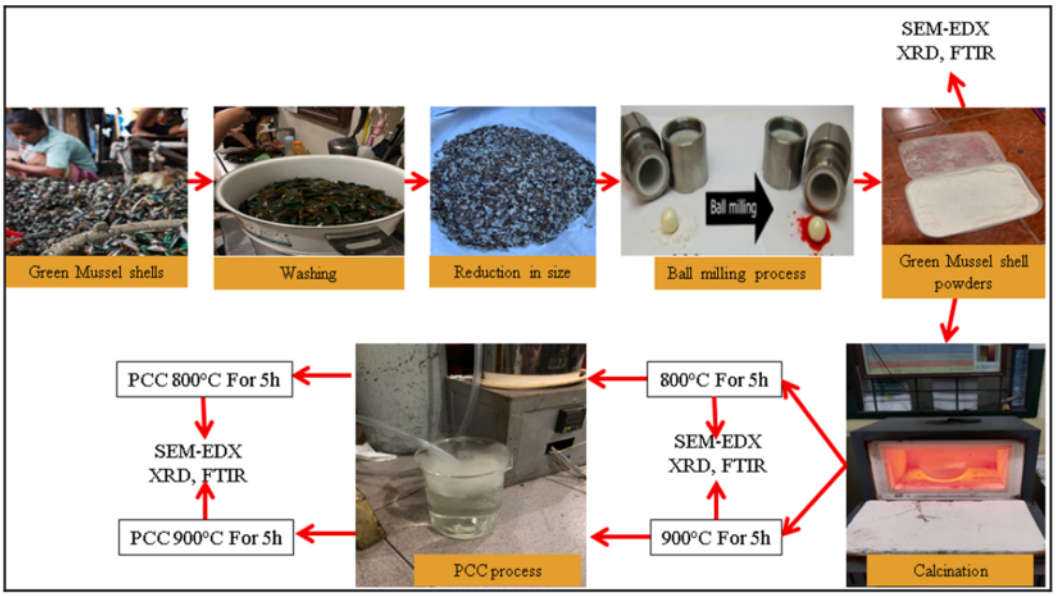

Fig. 1. Experimental setup for preparation of calcium carbonate from green mussel shells. (For interpretation of the references to color in this figure legend, the reader is referred to the web version of this article.)

Moreover, FTIR spectrometry (IR-Prestige88) was employed to examine the calcium carbonate formation of PCC products. All spectra at bands from 400 to 4000 cm^{-1} were recorded at 200 scans/s with a spectral of 2 cm^{-1} resolution.

3. Results & discussion

3.1. Quality and quantity of calcium carbonate powders

Samples of ground powder of green mussel shells, heat-treated ground powder, and PCC powder resulted from generated solutions were examined through a qualitative analysis of XRD data. In this way, intensity lines in XRD spectra were matched with those of the mineral database from the standard powder diffraction database (PDF) of the International Centre for Diffraction Data (ICDD) (PDF-2, ICDD-Release 2008). The determination of crystalline phases was then verified using the XRD Rietveld method. Fig. 2 shows XRD patterns of crystalline phases in all powder samples. The ground powder of green mussel shells shows the peak spectra of calcium carbonate with the highest intensity found at an angle of 2θ 26.233°, 27.238°, and 45.881°, which correspond to aragonite with the peaks matched with ICDD#PDF760606. The highest intensity spectra of XRD data for Cal-800 sample was found at an angle of 2θ 29.400°, 39.409°, and 48.505°, matching with the phases formed of calcite (ICDD#PDF831762) and portlandite ($Ca(OH)_2$) (ICDD#PDF 04–0733). In contrast to Cal-800 sample, Cal-900 sample has the XRD data with the highest intensity at an angle of 2θ 18.048°, 34.111° and 47.130° corresponding to the crystalline phase of portlandite. In the PCC-800 samples, the highest XRD peaks were identified

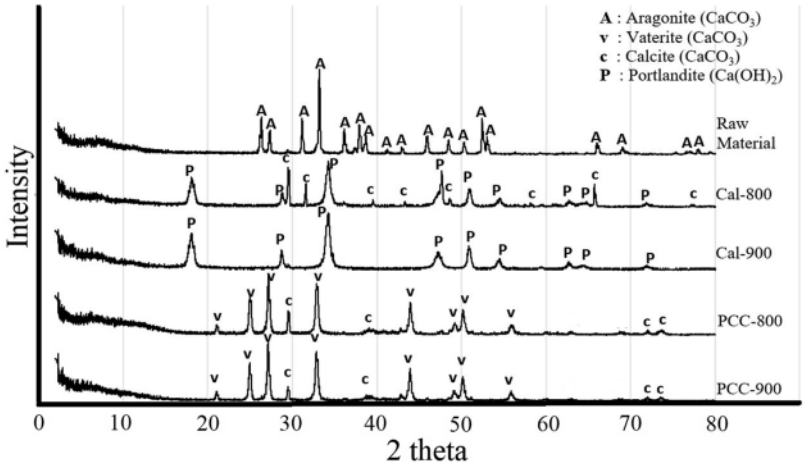

Fig. 2. X-ray diffractograms of shell powder, heat-treated powders at temperatures of 800 and 900 °C (Cal-800 and Cal-900), and PCC products (PCC-800 and PCC-900).

at an angle of 2θ 27.046°, 32.740° and 43.821° relating to the phases of vaterite (ICDD#PDF741867) and calcite. Similarly, the PCC-900 sample showing the highest intensity of XRD spectra was found at an angle of 2θ 27.1°, 32.8°, and 24.9° matched with phases of vaterite and calcite. All identified phases of those samples were then judged by the XRD Rietveld method confirming that the measured peak profiles of XRD data were well fitted with the peak profiles of standard XRD data. Fig. 3 presents for a plot of XRD Rietveld profile refinement for the PCC-900 sample.

Further, morphology and purity are significant variables of the processing and synthesis for calcium carbonates, while the amount of each phase grown represents an economic target of the powder processing strategy. In the study, the phase compositions of ground, heat-treated, and PCC powders were quantitatively derived by the XRD Rietveld method and the analysis results were given in Table 1. It was observed that in the experiment the raw material of green mussel shells is rich in aragonite. When the calcination was carried out at increasing temperatures (800 and 900 °C), the phase composition of the calcination product changed with temperature. Presumably, the calcination temperature made a decomposition of aragonite into calcite and portlandite. After the beginning of the calcination, aragonite seemed to decompose resulting in the minor calcite and high amount of portlandite at 800 °C. Nonetheless, there was no calcite formed and replaced by portlandite at a temperature of 900 °C. Based on the thermogravimetric analysis, calcium carbonate decomposition is reported to occur at a rising temperature from 600 °C to 800 °C. With the subsequent increasing temperature to reach 900 °C, the transformation of calcium carbonate attained equilibrium (almost completely transformation) [37]. Also, another study reported that the transformation temperature of the natural aragonite is about 450–500 °C, whereas the strong endothermic peak could be identified in the range of temperatures of 766.8–848.6 °C resulting in calcite decomposition [38]. With calcination of the samples was performed at temperatures of 800 and 900 °C, the present XRD analyses proved the result of an endothermic conversion from aragonite crystal to calcite and portlandite occurring in the calcined sample of Cal-800. Additionally, almost complete decomposition of aragonite to portlandite could be confirmed experiencing in the sample of Cal-900 (Table 1).

Obviously, the amount of portlandite increased with the progress of the calcination due to the release of the CO_2 at 800 and 900 °C, while more than 30% of weight loss of pure calcite occurred during the experimental synthesis (see Table 1). After the end of decomposition at calcination temperatures of 800 and 900 °C, the weight ratios of calcite versus portlandite in the product of calcium carbonate turned to be 33:67 and 0:100, respectively. These results confirmed that the total decomposition of calcium carbonate occurred in the sample of Cal-900 and implied the release of CO_2 from calcium carbonate resulting in only the product of portlandite. Accordingly, the large amount of

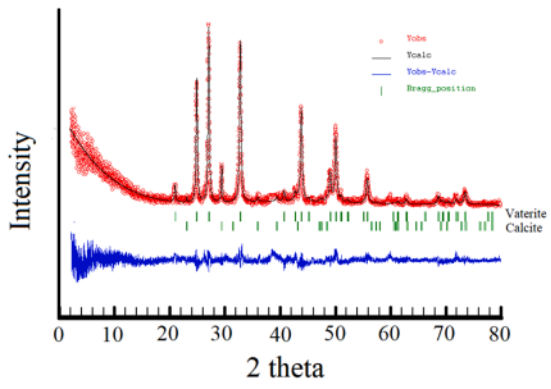

Fig. 3. XRD Rietveld plot of PCC-900 product.

Table 1
Crystalline phases of products from the ground powder of raw material, the calcined powders (Cal-800 and Cal-900), and the precipitating solid (PCC-800 and PCC-900).

Phase	Weight (%)				
	Raw Material	Cal-800	Cal- 900	PCC-800	PCC-900
Calcite	–	33.09(44)*	–	7.84(33)	8.74(70)
Aragonite	100	–	–		
Vaterite	–	–	–	92.16(98)	91.26(65)
Portlandite	–	66.91 (58)	100	–	–
Total	100.00	100.00	100.00	100.00	100.00

* The number in parenthesis indicates the standard deviations obtained from the XRD Rietveld quantitative analysis.

portlandite (~100 wt%) could be produced at the calcination temperature of 900 °C, which agreed with the result of thermogravimetric analysis in which the decomposition of calcium carbonate remained unchanged at the temperature reaching 900 °C [37,38].

Further synthesis factors influencing the formation of calcium carbonate polymorphs are in multiple and interacting ways, in that the temperatures of calcination strongly control the precipitation of each polymorph in the solution. Here the PCC resulting from the calcium carbonate solutions has a different phase composition at varying the CO_2 flow rates and calcination temperatures, in which the amounts of vaterite and calcite were controlled by temperature during the carbonation process. It was proposed that in the experiments the transformation from portlandite to vaterite and calcite proceeded in the solutions according to [28]:

$$Ca(OH)_2 + CO_2 \Rightarrow CaCO_3 + H_2O \quad (5)$$

Here the reaction pathways of the PCC from the powders of green mussel shells through mineral carbonation can somewhat counterbalance by the total cost of heating and the dissolution process. However, the particular use of green mussel shells as calcium sources for the fabrication of the PCC may provide the environmental benefits in terms of reuse and recycle of the marine wastes.

3.2. Chemical composition and morphology for powder samples

The chemical elements (wt.%) of all powders were obtained from EDX analysis and results are given in Table 2. This EDX data did not provide the actual form of chemical bonding present in the powder samples. However, oxides and carbonates are supposed to be the main chemical compounds of the powders. Obviously, powders of the green mussel shells mainly contain Ca, C, and O, in addition to small amount of Na-ion (0.5%). The major chemical components of these green mussel shells are rather alike to those of the commercial powder of calcium carbonate. After the calcination process, a change in the chemical compositions of the powders could not be observed during the study.

The only small variation of calcium content may be associated with the carbonation process. Furthermore, the calcination temperatures (from 800 to 900 °C) made reduced in Na content (0.21%) and finally

Table 2
EDX-based chemical elements of the ground powder of raw material, the calcined powders (Cal-800 and Cal-900) and the precipitating solid (PCC-800 and PCC-900), and commercial calcium carbonate.

Element	Mass (%)					
	Cal-800	Cal-900	PCC-800	PCC-900	Raw Material	Commercial $CaCO_3$
C	6.34	7.13	14.80	14.11	17.56	10.99
O	48.13	51.21	54.67	52.41	53.09	48.13
Na	0.21	–	–	–	0.50	–
Ca	45.33	41.66	30.53	33.48	28.85	40.88
Total	100.00	100.00	100.00	100.00	100.00	100.00

disappeared. Additionally, the Ca content in the PCC samples decreased due to carbonation by introducing CO_2 streams into the solution. Conversely, the carbonization process made an increase in the contents of C and O. Also, the increasing temperature made an increase in the CO_2 solubility within the solution [39,40]. Accordingly, vaterite was formed in the PCC samples because of directly reacting with CO_2 in the solution.

SEM images for morphologies of calcium carbonate powders made from green mussel shells, the calcination process of shells, and precipitating solution are shown in Fig. 4. Prior to calcination, green mussel shell powders with an irregular shape morphology could be observed to look like small branching stems of common aragonite crystals (Fig. 4a), while the commercial calcium carbonate has a cube-like shape morphology, which is commonly found in the calcite crystal (Fig. 4b) [41]. The crystalline phase of powders obtained at calcination of 800 °C (Cal-800) yielded a small cube-like shape morphology with irregular shapes. This morphological shape corresponds to the presence of 2 (two) crystalline phases in that sample, namely cube-like shape for calcite (Fig. 5a) and hexagonal-like shape for portlandite (Fig. 5b). Moreover, the main crystalline phase of portlandite produced at 900 °C has a more irregular hexagonal-like shape morphology compared to that in the sample obtained at 800 °C, which relates to the strong effect of temperature on change of morphology [42]. SEM images of the PCC-800 and PCC-900 samples show the small spherical-like shape morphology with sizes smaller than 5 μm, which relates a major vaterite crystal as confirmed by the XRD quantitative analysis (Fig. 6a-b; Table 1) [14]. As reported previously [43] the average particle size of calcium carbonate is typically between 1 and 3 μm those have resulted from a precipitation process at ambient temperature. Further, a difference in particle size between PCC-800 and PCC-900 samples could be identified in SEM images. Likely, changes in pH and the CO_2 concentration controlled the particle size in the course of the experimental study. As demonstrated previously [15,31,43], the particle size of calcium carbonate resulted from the precipitation related to the reduction in the CO_2 bubble size, and in the CO_2 concentration. However, further experimental work for controllable CO_2 bubbles and CO_2 concentrations is still required to understand the effects of reaction conditions on the product properties. Furthermore, the commercial $CaCO_3$ has a cube-like shape morphology, which is the characteristic of calcite [26].

3.3. FTIR analysis of powder samples

FTIR examinations of green mussel shells, heat-treated ground green mussel shells, precipitated calcium carbonate, and commercial $CaCO_3$ and their results are given in Fig. 7. Generally, a positional shift of peaks versus the reported standard peaks could be observed in all samples. This shift was possibly related to the presence of hydrogen bonding making a shift toward the lower frequency of all functional groups involving in hydrogen bonding [44]. In the study, FTIR spectra for calcium carbonate appeared at 864.1 and 711.14 cm^{-1} bands and at 1473.62 and 1392.22 cm^{-1} bands, which correspond to respective Ca-O and C-O bonds, matching with a high concentration of $CaCO_3$ as observed in the samples. The FTIR results can also characterize the types of crystals formed based on the characteristic of the resulting peaks. Prominent absorption bands in the range of 700–900 cm^{-1} could be assigned for aragonite in powder samples of commercial calcium carbonate and the mussel shells. Conversely, the low relative intensity bands at around 3400–3600 cm^{-1} corresponding to O-H bonds were confirmed in all samples except for the commercial calcium carbonate samples. Particularly, the O-H bond may be related to a low concentration of $Ca(OH)_2$ having a sharp band of 3641 cm^{-1}, which was possibly formed on the Cal-800 and Cal-900 samples, because of its hygroscopic property [45]. Also, the hydroxide may be a remaining ion formed during the calcination process. FTIR spectra at the band of 879.84 cm^{-1} appeared on samples (i.e. PCC-800 and PCC-900) corresponding to vaterite as confirmed by the previous XRD analyses [46].

3.4. Feasibility of green mussel as a starting biomaterial

Powder processing strategies of green mussel *Perna Viridis* shells for yielding the added-value of calcium carbonates have been demonstrated in the study. The obtained powder products exhibited varying polymorphic forms of calcium carbonates. Correspondingly, the calcium carbonates, or its derivatives from the powder processing procedures have been found to be potential for multipurpose usages [47]. Such a powder processing procedure has become a key aspect of the experimental study for preparing and converting of the green mussel shells into value-added calcium carbonate. The success level to produce calcium carbonate phases depending on the powder processing route, synthesis parameters, and drying method. In the study, the batch laboratory experiments performed with powders with varying particle sizes, the calcination temperature, and pH provided significant results for the quality and quantity of calcium carbonate products. A reasonable amount of aragonite (100 wt%) as confirmed by XRD phase composition analysis could be obtained by milling process of the green mussel shells

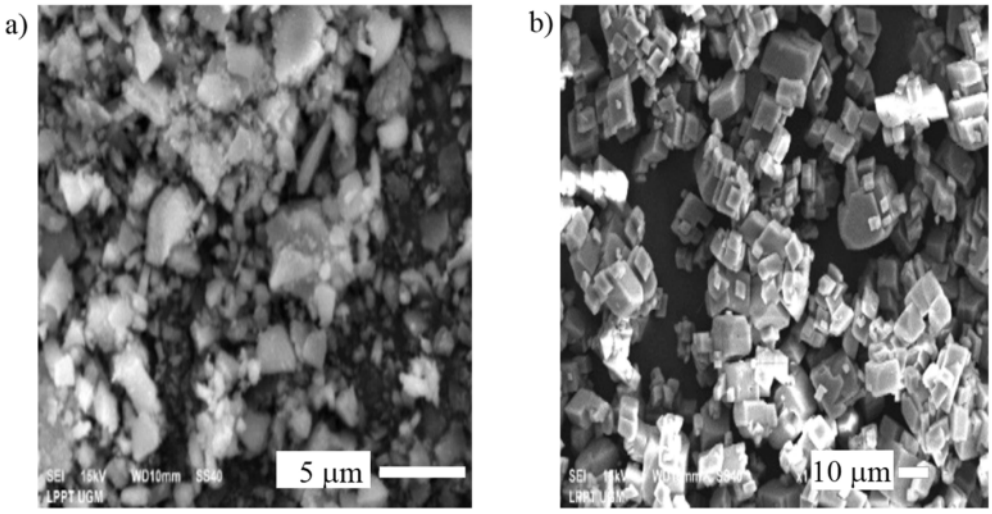

Fig. 4. SEM images of a) calcium carbonate made from green mussel shells and b) commercial $CaCO_3$.

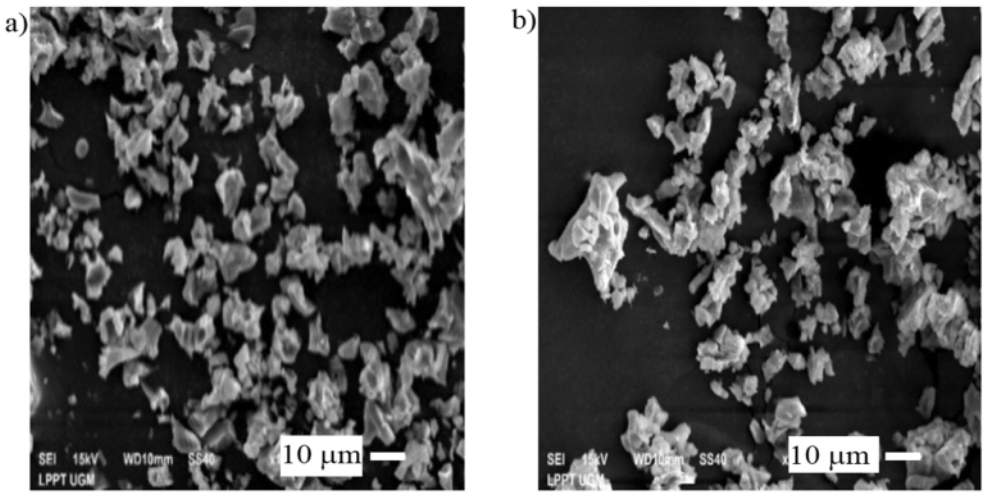

Fig. 5. SEM images of a) Cal-800 powder sample and b) Cal-900 powder sample.

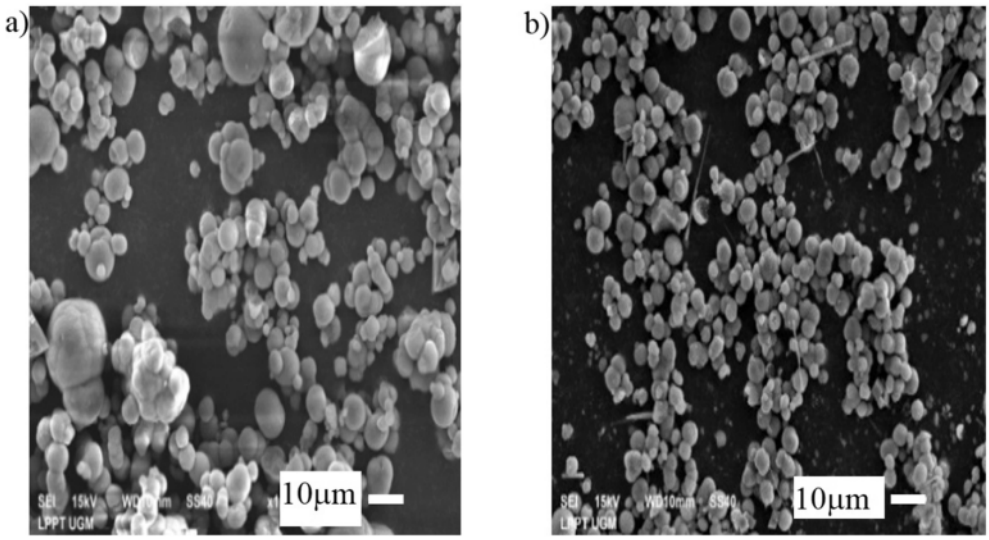

Fig. 6. SEM images of precipitated calcium carbonate for a) the PCC-800 and b) PCC-900 Samples.

as a starting material, while the calcination processes of these milled powders at 800 °C and 900 °C yielded the change of phase compositions in the calcium carbonate products along with varying morphologies and particle size. At the temperature of 900 °C, the selected temperature and reaction time may influence the formation of the pure portlandite phase with controlled morphology. Furthermore, the PCC with controlled morphology could be obtained by precipitation technique of the heat-treated ground powder as starting materials from the mixture of HNO_3 and NH_4OH solution. In this precipitation process, the resulted PCC powders had spherical particles with a size of <10 μm forming agglomeration with calcite and vaterite, though vaterite was still the major phase.

It was proposed that in the present synthesis the increase in the vaterite content in the PCC structure may be reached through increasing reaction time when the CO_2 stream kept in contact with the reaction solution. In addition, the resulted particle size and morphology may be controlled by the stirring rate in the precipitation process, in that synthetic vaterite particles have become a great concern about using them in vascular medicine. Vaterite is well known as biomedical because of its biocompatible [48] and low toxicity [49,50]. For the medical purpose, the high purity of vaterite with homogeneous spherical particles are vital for ensuring the marketability. These characteristic particles are required for attaining the degree of penetrance in the drug delivery to the lung [14,50,51]. In some cases, vaterite with particle size in the range of sizes of 300 nm to 6 μm can be simply governed in the powder processing procedures. In future work, the synthesis from the reactivity of PCC and H_3PO_4 would be described to yield the Ca-HA for medical use in the absence of impurities [52,53].

4. Conclusion

The results of this study demonstrated calcium carbonate

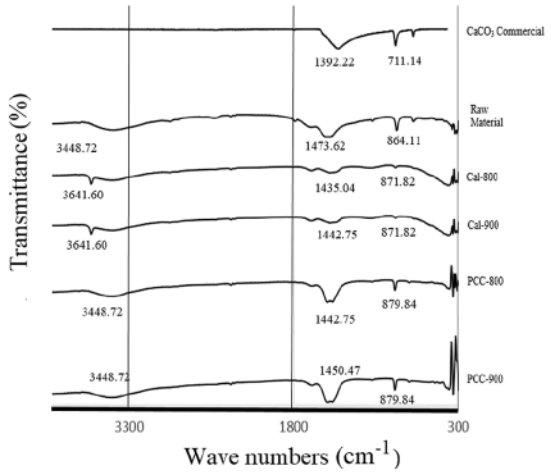

Fig. 7. FTIR spectra of $CaCO_3$ commercial, raw material, calcined (Cal-800 and Cal-900) powders, and PCC (PCC-800 and PCC-900) powders.

polymorphs obtained from the powder processing and calcination-dissolution-precipitation (CDP) technique of the green mussel shell powder. Based on the results of XRD, SEM-EDX, and FTIR evaluations, the heat-treating of the ground powder provided a high amount of portlandite and minor calcite in the Cal-800 sample, but calcite was totally lost leading to yield pure portlandite in the Cal-900 sample as a result of CO_2 release. Additionally, PCC product has the same characteristics as commercial $CaCO_3$. There is no different polymorph in the PCC product that was observed relating to the CO_2 stream in contact with the reaction solution. Importantly, the PCC-800 and PCC-900 products have a high content of vaterite which is a potential candidate biomaterial in a drug delivery system. The synthesis procedure of the PCC product resulted in calcium carbonate which can be used for a starting biomaterial of the high purity Ca-HA.

Credit authorship contribution statement

R. Ismail: Conceptualization, Writing-original draft, Investigation, Methodology. **D.F. Fitriyana:** Conceptualization, Writing-original draft, Data curation, Investigation, Methodology. **Y.I. Santosa:** Data curation. **S. Nugroho:** Formal analysis. **A.J. Hakim:** Formal analysis. **M.S. Al Mulqi:** Formal analysis. **J. Jamari** Funding aquisition, Project administration, Resources, software, supervision, validation, Visualisation, writing review & editing. **A.P. Bayuseno:** Conceptualization, writing-original draft, Resources, software, supervision, validation, Visualisation, writing review & editing.

Declaration of Competing Interest

The authors declare that they have no known competing financial interests or personal relationships that could have appeared to influence the work reported in this paper.

Acknowledgements

This research is partially funded by the Indonesian Ministry of Research and Technology/National Agency for Research and Innovation, and the Ministry of Education and Culture under World Class University (WCU) Program managed by Institut Teknologi Bandung and partially supported by Research Grant of International Publication provided by Diponegoro University Indonesia under contract of number: 258-22/UN7.P4.3/PP/2019.

References

[1] T.K. Soon, J. Ransangan, Feasibility of green mussel (Perna viridis) farming in Marudu Bay, Malaysia, Aquac. Rep. 4 (2016) 130–135, https://doi.org/10.1016/j.aqrep.2016.06.006.
[2] H.A.W. Cappenberg, Some aspects of the biology of green mussels (Perna viridis) Linnaeus 1758 Oseana, XXXIII(1), (2008) 33–40 (original in Indonesian).
[3] M.C. Barros, P.M. Bello, M. Bao, J.J. Torrado, From waste to commodity: transforming shells into high purity calcium carbonate, J. Clean. Prod. 17 (2009) 400–407, https://doi.org/10.1016/j.jclepro.2008.08.013.
[4] L.M.M. Costa, G.M. Olyveira, R. Salomão, Precipitated calcium carbonate nano-microparticles: applications in drug delivery, Adv. Tissue Eng. Regen Med. Open Access 3 (2017) 336–340, https://doi.org/10.15406/atroa.2017.03.00059.
[5] M.-C. Wan, W. Qin, C. Lei, Q.-H. Li, M. Meng, M. Fang, W. Song, J.-H. Chen, F. Tay, L.-N. Niu, Biomaterials from the sea: Future building blocks for biomedical applications, Bioact. Mater. 6 (2021) 4255–4285, https://doi.org/10.1016/j.bioactmat.2021.04.028.
[6] S. Kirboga, M. Oner, Effect of the experimental parameters on calcium carbonate precipitation, Chem. Eng. Trans. 32 (2013) 2119–2124, https://doi.org/10.3303/CET1332354.
[7] C. Yang, X. Yang, T. Zhao, F. Liu, An indirect CO2 utilization for the crystallization control of CaCO3 using alkylcarbonate, J. CO2 Util. 45 (2021), https://doi.org/10.1016/j.jcou.2021.101448.
[8] F. Liendo, M. Arduino, F.A. Deorsola, S. Bensaid, Optimization of $CaCO_3$ synthesis through the carbonation route in a packed bed reactor, Powder Technol. 377 (2021) 868–881, https://doi.org/10.1016/j.powtec.2020.09.036.
[9] Y.H. Leung, C.M.N. Chan, A.M.C. Ng, H.T. Chan, M.W.L. Chiang, A.B. Djurišić, Y. H. Ng, W.Y. Jim, M.Y. Guo, F.C.C. Leung, W.K. Chan, D.T.W. Au, Antibacterial activity of ZnO nanoparticles with a modified surface under ambient illumination, Nanotechnology 23 (2012) 1–12, https://doi.org/10.1088/0957-4484/23/47/475703.
[10] Y. Fujita, T. Yamamuro, T. Nakamura, S. Kotani, C. Ohtsuki, T. Kokubo, The bonding behavior of calcite to bone, J. Biomed. Mater. Res. 25 (1991) 991–1003, https://doi.org/10.1002/jbm.820250806.
[11] Y. Svenskaya, B. Parakhonskiy, A. Haase, V. Atkin, E. Lukyanets, D. Gorin, R. Antolini, Anticancer drug delivery system based on calcium carbonate particles loaded with a photosensitizer, Biophys. Chem. 182 (2013) 11–15, https://doi.org/10.1016/j.bpc.2013.07.006.
[12] D. Volodkin, $CaCO_3$ templated micro-beads and capsules for bioapplications, Adv. Colloid Interface Sci. 207 (2014) 306–324, https://doi.org/10.1016/j.cis.2014.04.001.
[13] S. Schmidt, D. Volodkin, Microparticulate biomolecules by mild $CaCO_3$ templating, J. Mater. Chem. B 1 (2013) 1210–1218, https://doi.org/10.1039/c2tb00344a.
[14] D.B. Trushina, T.V. Bukreeva, M.V. Kovalchuk, M.N. Antipina, $CaCO_3$ vaterite microparticles for biomedical and personal care applications, Mater. Sci. Eng. C 45 (2014) 644–658, https://doi.org/10.1016/j.msec.2014.04.050.
[15] L. Ma, L. Zhao, Y. Li, J. Zhang, Controllable crystallization of pure vaterite using CO2-storage material and different Ca2+ sources, J. CO2 Util. 48 (2021), https://doi.org/10.1016/j.jcou.2021.101520.
[16] J. Küther, R. Seshadri, W. Knoll, W. Tremel, Templated growth of calcite, vaterite and aragonite crystals on self-assembled monolayers of substituted alkylthiols on gold, J. Mater. Chem. 8 (1998) 641–650, https://doi.org/10.1039/a705859d.
[17] C. Wang, J. Zhao, X. Zhao, H. Bala, Z. Wang, Synthesis of nanosized calcium carbonate (aragonite) via a polyacrylamide inducing process, Powder Technol. 163 (3) (2006) 134–138, https://doi.org/10.1016/j.powtec.2005.12.019.
[18] J. Chen, L. Xiang, Controllable synthesis of calcium carbonate polymorphs at different temperatures, Powder Technol. 189 (2009) 64–69, https://doi.org/10.1016/j.powtec.2008.06.004.
[19] Z.P. Xu, Q.H. Zeng, G.Q. Lu, A.B. Yu, Inorganic nanoparticles as carriers for efficient cellular delivery, Chem. Eng. Sci. 61 (3) (2006) 1027–1040, https://doi.org/10.1016/j.ces.2005.06.019.
[20] G. Magnabosco, D. Giuri, A.P.D. Bisceglie, F. Scarpino, S. Fermani, C. Tomasini, G. Falini, New material perspective for waste seashells by covalent functionalization, ACS Sustainable Chem. Eng. 9 (2021) 6203–6208, https://doi.org/10.1021/acssuschemeng.1c01306.
[21] N.A. Oladoja, I.A. Ololade, A.O. Adesina, R.O.A. Adelagun, Y.M. Sanic, Appraisal of gastropod shell as calcium ion source for phosphate removal and recovery in calcium phosphate minerals crystallization procedure, Chem. Eng. Res. Des. 91 (5) (2013) 810–818, https://doi.org/10.1016/j.cherd.2012.09.017.
[22] Kh.N. Islam, Md.Z.B. Abu Bakar, M.M. Noordin, M.Z.B. Hussein, N.S. B. AbdRahman, Md.E. Ali, Characterisation of calcium carbonate and its polymorphs from cockle shells (Anadara granosa), Powder Technol. 213 (1–3) (2011) 188–191, https://doi.org/10.1016/j.powtec.2011.07.031.
[23] J.N. Murphy, K. Hawboldt, F.M. Kerton, Enzymatic processing of mussel shells to produce biorenewable calcium carbonate in seawater, Green Chem. 20 (2018) 2913–2920, https://doi.org/10.1039/c8gc01274a.
[24] B. Viswanath, N. Ravishankar, Controlled synthesis of plate-shaped hydroxyapatite and implications for the morphology of the apatite phase in bone, Biomaterials 29 (36) (2008) 4855–4863, https://doi.org/10.1016/j.biomaterials.2008.09.001.
[25] J.W. Morse, A.J. Andersson, F.T. Mackenzie, Initial responses of carbonate-rich shelf sediments to rising atmospheric pCO2 and "ocean acidification'': Role of high Mg-calcites, Geochim. Cosmochim. Acta 70 (2006) 5814–5830, https://doi.org/10.1016/j.gca.2006.08.017.
[26] M.R.R. Hamester, P.S. Balzer, D. Becker, Characterization of calcium carbonate obtained from oyster and mussel shells and incorporation in polypropylene, Mater.

Res. 15 (2) (2012) 204–208, https://doi.org/10.1590/S1516-14392012005000014.
[27] H. Zhao, Y. Park, D.H. Lee, A.H.A. Park, Tuning the dissolution kinetics of wollastonite via chelating agents for CO_2 sequestration with integrated synthesis of precipitated calcium carbonates, Phys. Chem. Chem. Phys. 15 (2013) 15185–15192, https://doi.org/10.1039/C3CP52459K.
[28] R. Chang, S. Kim, S. Lee, S. Choi, M. Kim, Y. Park, Calcium carbonate precipitation for CO_2 storage and utilization: A Review of the carbonate crystallization and polymorphism, Front. Energy Res. 5 (17) (2017) 1–12, https://doi.org/10.3389/fenrg.2017.00017.
[29] Y. Azis, N. Jamarun, S. Zultiniara, H. Nur Arief, Synthesis of hydroxyapatite by hydrothermal method from cockle shell (Anadara granosa), J. chem. pharm 7 (5) (2015) 798–804.
[30] C. Ramakrishna, T. ThriveniThenepalli, C. ChoonHan, J.W. Ahn, Synthesis of aragonite-precipitated calcium carbonate from oyster shell waste via a carbonation process and its applications, Korean J. Chem. Eng. 34 (1) (2017) 225–230, https://doi.org/10.1007/s11814-016-0264-6.
[31] C. Martos, B. Coto, J.L. Pena, R. Rodríguez, D. Merino-Garcia, G. Pastor, Effect of precipitation procedure and detection technique on particle size distribution of CaCO3, J. Cryst. Growth 312 (2010) 2756–2763, https://doi.org/10.1016/j.jcrysgro.2010.06.006.
[32] J. Rodriguez-Carvajal, Program Fullprof.2k, version 3.30, Laboratoire Leon Brillouin, France, June 2005.
[33] R.T. Downs, M. Hall-Wallace, The American mineralogist crystal structure database, American Mineralogist 88 (2003) 247.
[34] R.J. Hill, C.J. Howard, Quantitative phase analysis from neutron powder diffraction data using the Rietveld method, J. Appl. Crystallogr. 20 (1987) 467–474, https://doi.org/10.1107/S0021889887086199.
[35] A.P. Bayuseno, W.W. Schmahl, Hydrothermal synthesis of struvite and its phase transition: Impacts of pH, heating and subsequent cooling methods, J. Cryst. Growth 498 (15) (2018) 336–345, https://doi.org/10.1016/j.jcrysgro.2018.06.026.
[36] P.Y. Mahieux, J.E. Aubert, M. Cyr, M. Coutand, B. Husson, Quantitative mineralogical composition of complex mineral wastes–contribution of the Rietveld method, Waste Manage. 30 (2010) 378–388, https://doi.org/10.1016/j.wasman.2009.10.023.
[37] A.S. Kamba, M. Ismail, T.A.T. Ibrahim, Z.A.B. Zakaria, 2013) Synthesis and Characterisation of Calcium Carbonate Aragonite Nanocrystals from Cockle Shell Powder (Anadara granosa, J. Nanomater (2013), https://doi.org/10.1155/2013/398357.
[38] F.Z. Ren, X.D. Wan, Z.H. Ma, J.H. Su, Study on Microstructure and Thermodynamics of Nacre in Mussel Shell, Mater. Chem. Phys. 114 (2009) 367–370, https://doi.org/10.1016/j.matchemphys.2008.09.036.
[39] T. Zhao, B. Guo, F. Zhang, F. Sha, Q. Li, J. Zhang, Morphology control in the synthesis of $CaCO_3$ microspheres with a novel CO_2 storage material, ACS Appl. Mater. Interfaces 7 (2015) 15918–15927, https://doi.org/10.1021/acsami.5b03568.
[40] L. Xiang, Y. Xiang, Y. Wen, F. Wei, Formation of $CaCO_3$ nanoparticles in the presence of terpineol, Mater. Lett. 58 (6) (2004) 959–965, https://doi.org/10.1016/j.matlet.2003.07.034.
[41] M. Pacton, P. Sorrel, B. Bevillard, A. Zacai, A. Vincon-Laugier, H. Oberhansli, Sedimentary facies analyses from nano to millimetre scale exploring past microbial activity in a high-altitude lake (Lake Son Kul, Central Asia), Geol. Mag. 152 (5) (2015) 902–922, https://doi.org/10.1017/S0016756814000831.
[42] J. Jiang, Q. Qi Zheng, D. Hou, Y. Yan, H. Heng Chen, W. Wei She, S. Wu, D. Guod, W. Sun, Calcite crystallization in the cement system: Morphological diversity, growth mechanism and shape evolution, Phys. Chem. Chem. 20 (20) (2018) 14174–14181, https://doi.org/10.1039/c8cp01979g.
[43] B. Feng, A.K. Yong, H. An, Effect of various factors on the particle size of calcium carbonate formed in a precipitation process, Mater. Sci. Eng. A 445–446 (2007) 170–179, https://doi.org/10.1016/j.msea.2006.09.010.
[44] N.V. Vagenas, A. Gatsouli, C.G. Kontoyannis, Quantitative analysis of synthetic calcium carbonate polymorphs using FT-IR spectroscopy, Talanta 59 (2003) 831–836, https://doi.org/10.1016/S0039-9140(02)00638-0.
[45] N. Koga, Y. Nakagoe, H. Tanaka, Crystallization of amorphous calcium carbonate, Thermochim. Acta 318 (1998) 239–244, https://doi.org/10.1016/S0040-6031(98)00348-7.
[46] E. Lostea, R.M. Wilson, R. Seshadric, F.C. Meldrum, The role of magnesium in stabilising amorphous calcium carbonate and controlling calcite morphologies, J. Cryst. Growth 254 (2003) 206–218, https://doi.org/10.1016/S0022-0248(03)01153-9.
[47] A.L. Goodwin, F. Marc Michel, L. Brian, B.L. Phillips, D.A. Keen, T. Martin, M. T. Dove, R.J. Reeder, Nanoporous Structure and Medium-Range Order in Synthetic Amorphous Calcium Carbonate, Chem. Mater. 22 (10) (2010) 3197–3205, https://doi.org/10.1021/cm100294d.
[48] S. Biradar, P. Ravichandran, R. Gopikrishnan, V. Goornavar, J.C. Hall, V. Ramesh, S. Baluchamy, R.B. Jeffers, G.T. Ramesh, Calcium carbonate nanoparticles: synthesis, characterization and biocompatibility, J. Nanosci. Nanotechnol. 11 (8) (2011) 6868–6874, https://doi.org/10.1166/jnn.2011.4251.
[49] B. Parakhonskiy, M.V. Zyuzin, A. Yashchenok, S. Carregal-Romero, J. Rejman, H. Möhwald, W.J. Parak, A.G. Skirtach, The influence of the size and aspect ratio of anisotropic, porous $CaCO_3$ particles on their uptake by cells, J. Nanobiotechnol. 13 (53) (2015) 1–13, https://doi.org/10.1186/s12951-015-0111-7.
[51] Y.I. Svenskaya, A.M. Pavlov, D.A. Gorin, D.J. Gould, B.V. Parakhonskiy, G. B. Sukhorukov, Photodynamic therapy platform based on localized delivery of photosensitizer by vaterite submicron particles, Colloids and Surf. B Biointerfaces 146 (2016) 171–179, https://doi.org/10.1016/j.colsurfb.2016.05.090.
[52] D. Volodkin, $CaCO_3$ templated micro beads and capsules for bioapplications, Adv. Colloid Interface Sci. 207 (2014) 306–324, https://doi.org/10.1016/j.cis.2014.04.001.
[53] D.P. Minh, S. Rio, P. Sharrock, H. Sebei, N. Lyczko, N.D. Tran, M. Raii, A. Nzihou, Hydroxyapatite starting from calcium carbonate and orthophosphoric acid: synthesis, characterization, and applications, J. Mater. Sci. 49 (2014) 4261–4269, https://doi.org/10.1007/s10853-014-8121-7.

The potential use of green mussel (Perna Viridis) shells for synthetic calcium carbonate polymorphs in biomaterials

ORIGINALITY REPORT

13%	9%	12%	4%
SIMILARITY INDEX	INTERNET SOURCES	PUBLICATIONS	STUDENT PAPERS

MATCH ALL SOURCES (ONLY SELECTED SOURCE PRINTED)

1%

★ real.mtak.hu

Internet Source

Exclude quotes	On	Exclude matches	Off
Exclude bibliography	On		

The potential use of green mussel (Perna Viridis) shells for synthetic calcium carbonate polymorphs in biomaterials

GRADEMARK REPORT

FINAL GRADE

/1

GENERAL COMMENTS

Instructor

PAGE 1

PAGE 2

PAGE 3

PAGE 4

PAGE 5

PAGE 6

PAGE 7

PAGE 8